Available online at www.sciencedirect.com
SCIENCE DIRECT®
Journal of Sound and Vibration 276 (2004) 227–244
JOURNAL OF SOUND AND VIBRATION
www.elsevier.com/locate/jsvi

Damage localization in plate structures from uniform load surface curvature

D. Wu, S.S. Law*

Department of Civil and Structural Engineering, Hong Kong Polytechnic University, Hung Hom, Hong Kong, China

Received 14 April 2003; accepted 25 July 2003

Abstract

Although a large number of methods exist for detecting damage in a structure using measured modal parameters, many of them require a correlated finite element model, or at least, modal data of the structure for the intact state as baseline. For one-dimensional beam-like structures, curvature techniques, e.g., mode shape curvature and flexibility curvature, have been applied to localize damage. In this paper a damage localization method based on changes in uniform load surface (ULS) curvature is developed for two-dimensional plate structures. A new approach to compute the ULS curvature is proposed based on the Chebyshev polynomial approximation, instead of the central difference method. The proposed method requires only the frequencies and mode shapes of the first few modes of the plate before and after damage, or only the eigenpairs for the damaged state if a gapped-smoothing technique is applied. Numerical simulations considering different supported conditions, measurement noise, mode truncation, and sensor sparsity are studied to evaluate the effectiveness of the proposed method. It is found that the ULS curvature is sensitive to the presence of local damages, even with truncated, incomplete, and noisy measurements.

1. Introduction

Damage generally produces changes in the structural physical properties (i.e., stiffness, mass, and damping), and these changes are accompanied by changes in the modal characteristics of the structure (i.e., natural frequencies, mode shapes, and modal damping). This phenomenon has been widely noted and used by structural engineers for detecting damage or health monitoring of a structure. Doebling et al. [1] provided an excellent review on research advances in this area over the last 30 years, and summarized this kind of technology as vibration-based damage identification methods.

*Corresponding author. Tel.: +852-2766-6062; fax: +852-2334-6389.
E-mail address: cesslaw@polyu.edu.hk (S.S. Law).

0022-460X/$ - see front matter © 2003 Published by Elsevier Ltd.
doi:10.1016/j.jsv.2003.07.040

According to the process to treat the measured modal parameters, the vibration-based damage identification methods can be classified as model based and non-model based. The model-based methods identify damage by correlating an analytical model, which is usually based on the finite element theory, with test modal data of the damaged structure [2–4]. Comparisons of the updated model to the original one provide an indication of damage and further information on the damage location and/or its extent. However, the construction of the finite element model usually gives rise to model errors from simplified assumptions. To detect the damage other than the artificial errors from the model construction, a good quality finite element model that could accurately depict the intact structure is required but is often difficult to achieve.

Non-model-based damage detection methods, also named as damage index methods, are relatively straightforward. The changes of modal parameters between the intact and damaged states of the structure are directly used, or correlated with other relevant information, to develop the damage indicators for localizing damage in the structure. Early works of damage index methodology make use of the natural frequency and mode shape information. Shifts in the natural frequencies [5], changes in the modal assurance criteria (MAC) across sub-structures [6], changes in the co-ordinate modal assurance criterion (COMAC) [7], and changes in the multiple damage location assurance criterion (MDLAC) [8] between the intact and damaged structure are formulated as indicators to localize damage. Pandey et al. [9] further demonstrated that changes in mode shape curvature could be a good indicator of damage for beam structures.

During the last decade, some researchers found that the modal flexibility can be a more sensitive parameter than natural frequencies or mode shapes alone for structural damage on detection. Raghavendrachar and Aktan [10] examined the application of modal flexibility for a three span concrete bridge. In their comparison with natural frequency and mode shapes, the modal flexibility is reported to be more sensitive and reliable for local damages. Zhao and Dewolf [11] presented a theoretical sensitivity study comparing the use of natural frequencies, mode shapes, and model flexibility for structural damage detection. The results demonstrate that modal flexibility is more likely to indicate damage than either the other two. Pandey and Biswas [12] proposed a damage localization method based on directly examining the changes in the measured modal flexibility of a beam structure. Lu et al. [13] pointed out that Pandey's method is difficult to locate multiple damages, and they recommended the modal flexibility curvature for multiple damage localization due to its high sensitivity to closely distributed structural damages.

Zhang and Aktan [14] comparatively studied the modal flexibility and its derivative, called uniform load surface (ULS), for their truncation effect and sensitivity to experimental errors. They suggested that the ULS has much less truncation effect and is least sensitive to experimental errors. These features make it a potentially useful index for experimental non-destructive evaluation.

So far most structural damage index methods are formulated in one-dimensional space, and therefore they can only be applied to beam-like structure or two-dimensional structures that can be decomposed into beam elements. In this paper, the uniform load surface curvature is proposed as a new local damage indicator due to its high sensitivity to damage with less experimental error effect. The curvature will be formulated using both the central difference method and the Chebyshev polynomial approximation, which are generalized to the two-dimensional space for plate structures. Damage can then be detected by investigating the curvature changes between the intact and damaged state, or from only the damaged state when a gapped-smoothing technique is

applied. Numerical simulations considering different supported conditions, measurement noise, mode truncation, and sensor sparsity are performed to demonstrate the effectiveness of the proposed method.

2. Theory

2.1. Definition of the uniform load surface

For a structural system with n degrees-of-freedom (d.o.f.), the flexibility matrix can be expressed by superposition of the mass normalized modes ϕ_r as [15]

$$F = \sum_{r=1}^{n} \frac{\phi_r \phi_r^{\mathrm{T}}}{\omega_r^2}, \tag{1}$$

where ω_r is the rth natural frequency. It can be seen from Eq. (1) that the modal contribution to the flexibility matrix decreases rapidly as the frequency ω_i increases, so the flexibility matrix converges rapidly as the number of contributing lower modes increases. This observation provides a great possibility to approximate closely the flexibility matrix with several lower modes.

In practice, indeed, there are only several, in most cases, two to three lower vibration modes of a structure which can be obtained with confidence from modal testing. When m lower modes are available, the modal flexibility matrix of the structure can be approximated as

$$F_T = [f_{k,l}] = \sum_{r=1}^{m} \frac{\phi_r \phi_r^{\mathrm{T}}}{\omega_r^2} \tag{2}$$

in which the modal flexibility, $f_{k,l}$, at the kth point under the unit load at point l is the summation of the products of two related modal coefficients for each available mode:

$$f_{k,l} = \sum_{r=1}^{m} \frac{\phi_r(k)\phi_r(l)}{\omega_r^2}. \tag{3}$$

For a linear system, the modal deflection at point k under uniform unit load all over the structure can be approximated as

$$u(k) = \sum_{l=1}^{n} f_{k,l} = \sum_{r=1}^{m} \frac{\phi_r(k)\sum_{l=1}^{n} \phi_r(l)}{\omega_r^2}. \tag{4}$$

The ULS is defined as the deflection vector of the structure under uniform load [14]

$$U_T = \{u(k)\} = F_T \cdot L, \tag{5}$$

where $L = \{1, \ldots, 1\}_{1\times n}^{\mathrm{T}}$ is the unit vector representing the uniform load acting on the structure. From Eqs. (3) and (4), Zhang and Aktan observed two features of the ULS comparative to the modal flexibility. Firstly, the ULS is less sensitive to measurement noise than the modal flexibility, because the summation of all the modal coefficients of the corresponding mode, $\sum_{l=1}^{n} \phi_r(l)$ in Eq. (4), averages out the random error at each measuring point. The second feature is that the ULS converges more rapidly with the lower modes than the modal flexibility. This is also because of the summation of all the modal coefficients of each mode to the ULS in Eq. (4). Since

the modal coefficients of higher modes tend to cancel each other more than those of the lower modes, the lower modes tend to contribute more than the higher modes to the ULS coefficients. This canceling effect does not exist with the modal flexibility formulation in Eq. (3). These significant properties make the ULS a potentially stable and sensitive damage indicator for structural health monitoring.

2.2. ULS curvature based on central difference method

Starting from this section we will focus on the damage detection with plate-like structures. It is assumed that the dynamic response of the plate is acquired by placing sensors in a rectangular grid, so that the mode shapes, and then the ULS can be estimated. In the absence of damage, the ULS of the plate is a smooth surface over the loading plane. When there is a fault, sharp changes in the ULS, like a peak or abrupt slope, will appear at the fault location. Based on the study of damage detection with mode shapes and flexibility for beam-like structures [9,13], the curvature technique is proven to be most efficient to locate these changes in the smooth curves. This technique is now generalized for the plate structures characterized by two-dimensional ULS curvature.

So far all the reported study on curvature-based damage detection computed the curvatures using a finite central differentiation procedure. When this technique is incorporated with two-dimensional ULS, the curvatures of the ULS are calculated by a Laplacian operator in each normal direction along the sensor grid as

$$u_{xx}(x_i, y_j) = \frac{u(x_{i+1}, y_j) - 2u(x_i, y_j) + u(x_{i-1}, y_j)}{h_x^2}, \tag{6a}$$

$$u_{yy}(x_i, y_j) = \frac{u(x_i, y_{j+1}) - 2u(x_i, y_j) + u(x_i, y_{j-1})}{h_y^2}, \tag{6b}$$

in which the ULS is grouped from a vector into a matrix according to the co-ordinates of measuring points in the grid, and the grid is assumed to be equally spaced in the x and y directions. h_x, h_y are the uniform grid spacings in the corresponding directions.

If two sets of measurements, one from the intact structure and the other from the damaged structure, are taken and the modal parameters are estimated from the measurements, the ULS curvature at point (x_i, y_j) for the two states can be obtained using Eqs. (4) and (6). The presence of the irregularity in the damaged curvature can be detected by subtracting the ULS curvature of the intact state from the curvature of the damaged state. Thereby a map of damage index can be formulated as follows:

$$d(x_i, y_j) = [\alpha_{xx}|u_{xx}^D(x_i, y_j) - u_{xx}(x_i, y_j)| + \alpha_{yy}|u_{yy}^D(x_i, y_j) - u_{yy}(x_i, y_j)|]^2, \tag{7}$$

where $|\cdot|$ denotes the absolute value, u_{xx}, u_{yy} are the measured ULS curvature values of the intact structure at the corresponding point along the x and y directions, respectively, and u_{xx}^D, u_{yy}^D are those of the suspected damaged structure. α_{xx} and α_{yy} are the weights that can be set from 0 to 1 to consider the importance of the curvature in the corresponding directions.

If the structure is undamaged when the second set of measurement is carried out, the difference between the two sets of measured ULS curvature would be due to measurement noise only.

Therefore values of the damage index map, $d(x_i, y_j)$, slightly oscillate around zero without any distinct peak. In contrast, if the structure is damaged, peaks or slopes will clearly show up at the damaged zone of the plate, as shown in the following numerical study.

2.3. ULS curvature based on Chebyshev polynomial approximation

The accuracy of the central difference method is well known depending on the density of the measurement grid. If the ULS values are estimated on a sparse grid, it will induce a very large error in calculating the curvature from differentiation. The following Chebyshev polynomial in two variables is adopted to model the ULS distribution so as to avoid this error:

$$u(x,y) = \sum_{i=1}^{N} \sum_{j=1}^{M} C_{ij} T_i(x) T_j(y), \tag{8}$$

where $T_i(x)$, $T_j(y)$ are the first kind Chebyshev polynomials, and N, M are their orders. To map the standard Chebyshev polynomials from the plane domain of $\{\xi, \mu\} = [-1, 1] \times [-1, 1]$ to the physical plate domain of $\{x, y\} = [0, L_x] \times [0, L_y]$, two linear transfer functions are defined

$$\xi = 2x/L_x - 1, \quad \mu = 2y/L_y - 1, \tag{9}$$

where L_x and L_y are the dimensions of the plate in the x and y directions, respectively. The Chebyshev polynomials of variable x is then written as

$$\begin{aligned} T_1(x) &= \frac{1}{\sqrt{\pi}}, \quad T_2(x) = \sqrt{\frac{2}{\pi}} \left(\frac{2x}{L_x} - 1 \right), \\ T_{i+1}(x) &= 2 \left(\frac{2x}{L_x} - 1 \right) T_i(x) - T_{i-1}(x), \quad i = 2, 3, \ldots, N-1. \end{aligned} \tag{10}$$

The polynomials of variable y can be formulated similarly.

Without loss of generality, it is assumed that $P = N \times M$ measuring points are set on the rectangular sensor grid so that the ULS can be estimated at these points. Eq. (8) will be satisfied at all the measuring points, and the Chebyshev polynomial approximation can be written in a matrix form

$$\{u(x_i, y_j)\}_{P \times 1} = [T(x_i) T(y_j)]_{P \times P} \{c_{ij}\}_{P \times 1}. \tag{11}$$

The coefficient vector $\{c_{ij}\}$ can then be solved as

$$\{c_{ij}\}_{P \times 1} = [T(x_i) T(y_j)]^{-1}_{P \times P} \{u(x_i, y_j)\}_{P \times 1} \tag{12}$$

or obtained by the least squares method if the number of measuring points $Q > P$:

$$\begin{aligned} \{c_{ij}\}_{P \times 1} = &([T(x_i) T(y_j)]^{\mathrm{T}}_{Q \times P} [T(x_i) T(y_j)]_{Q \times P})^{-1} \\ &\times [T(x_i) T(y_j)]^{\mathrm{T}}_{Q \times P} \{u(x_i, y_j)\}_{Q \times 1}. \end{aligned} \tag{13}$$

It is a better choice to have the measuring points at the Chebyshev zeros $(\hat{x}_i, \hat{y}_j)$, which ensure the convergence for any continuous function that satisfies a Dini–Lipschitz condition [16]. The

location of these $N \times M$ zeros is given by

$$\hat{x}_i = \left(\cos\frac{(i-0.5)\pi}{N} + 1\right)\frac{L_x}{2}, \quad i = 1, \ldots, N, \tag{14a}$$

$$\hat{y}_j = \left(\cos\frac{(j-0.5)\pi}{M} + 1\right)\frac{L_y}{2}, \quad j = 1, \ldots, M. \tag{14b}$$

The corresponding coefficients can be explicitly obtained as

$$c_{ij} = \frac{\lambda}{P}\sum_{r=1}^{N}\sum_{s=1}^{M} u(\hat{x}_i, \hat{y}_j)\cos\left(\frac{i(r-0.5)\pi}{N}\right)\cos\left(\frac{j(s-0.5)\pi}{M}\right) \begin{Bmatrix} i = 1, \ldots, N, \ j = 1, \ldots, M \\ r = 1, \ldots, N, \ s = 1, \ldots, M \end{Bmatrix}, \tag{15}$$

where

$$\lambda = \begin{cases} 1 & \text{for } i = 1, j = 1, \\ 2 & \text{for } i = 1, j \neq 1 \text{ or } i \neq 1, j = 1, \\ 4 & \text{for } i \neq 1, j \neq 1. \end{cases}$$

By making use of the orthogonal property of Chebyshev polynomial, the curvature of the ULS can then be approximated by the second derivatives of the Chebyshev polynomials in Eq. (8) as

$$u_{xx}(x, y) = \sum_{i=1}^{N}\sum_{j=1}^{M} c_{ij}\frac{\partial T_i^2(x)}{\partial x^2}T_j(y), \quad u_{yy}(x, y) = \sum_{i=1}^{N}\sum_{j=1}^{M} c_{ij}T_i(x)\frac{\partial T_j^2(y)}{\partial y^2} \tag{16a}$$

and

$$u_{xy}(x, y) = \sum_{i=1}^{N}\sum_{j=1}^{M} c_{ij}\frac{\partial T_i(x)}{\partial x}\frac{\partial T_j(y)}{\partial y}. \tag{16b}$$

Therefore, the formulation of the damage index in Eq. (7) can be rewritten as follows:

$$d(x_i, y_j) = [\alpha_{xx}|u_{xx}^D - u_{xx}| + \alpha_{yy}|u_{yy}^D - u_{yy}| + \alpha_{xy}|u_{xy}^D - u_{xy}|]^2. \tag{17}$$

2.4. The gapped-smoothing technique for plates

Most damage index methods require the "footprint", or baseline data set, of the intact structure for comparison to inspect the change in modal parameters due to damage. Typically, the "footprint" is obtained either from measurements of the undamaged structure, or from a finite element model of the intact structure. An inaccurate finite element model can bring in large model errors, and degrade or even lead to incorrect result in the damage detection. On the other hand, most suspected damaged civil structures were constructed several decades ago, and the "footprint" of the structures in the intact state is not available. To avoid this difficulty, Ratcliffe and Bagaria [17] proposed the "gapped-smoothing" technique with modal curvature, which allows the damage detection in a beam structure without prior knowledge on the undamaged

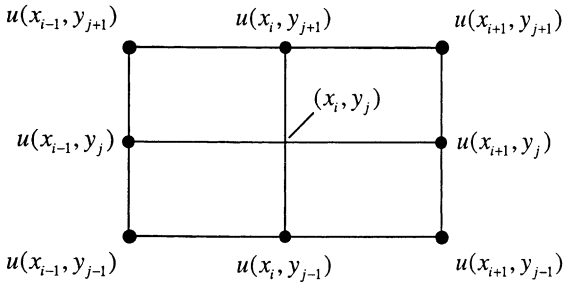

Fig. 1. Gapped grid for curve fitting at measuring point (x_i, y_j).

state. The "gapped-smoothing" technique is now extended and applied to bi-dimensional ULS curvature for the plate structures.

The basic idea of the method is that the ULS curvature of the plate, without any damage, has a smooth surface, and it can be approximated by a cubic polynomial in two variables:

$$\tilde{u}(x, y) = c_0 + c_1 x + c_2 y + c_3 x^2 + c_4 y^2 + c_5 xy + c_6 x^2 y + c_7 xy^2, \tag{18}$$

where the coefficients c_i can be evaluated by a curve-fitting process on the estimated ULS curvature of the damaged structure on a gapped grid of measuring points as shown in Fig. 1. Particularly, to obtain the smoothed ULS curvature at point (x_i, y_j), curvature data at all the adjacent points, but not the point (x_i, y_j) itself, are used to evaluate the coefficients c_i. This process is repeated for each measuring point to give a smooth ULS curvature to model the undamaged plate structure.

The presence of the peak in the ULS curvature due to local damage can then be detected by subtracting the smoothed curvature from the estimated curvature of the damaged structure. The damage index map is given similar to Eq. (17) as

$$d(x_i, y_j) = [\alpha_{xx}|u^D_{xx} - \tilde{u}_{xx}| + \alpha_{yy}|u^D_{yy} - \tilde{u}_{yy}| + \alpha_{xy}|u^D_{xy} - \tilde{u}_{xy}|]^2. \tag{19}$$

3. Numerical examples

Two plates with different boundary conditions, namely a four-side simply supported plate and a cantilever plate, are used as examples to demonstrate how the change in the ULS curvature can be used as index to locate damage in a plate. These examples were chosen because each of them exhibits different behavior with the load distribution. For example, in a uniformly loaded four-side simply supported plate, both the maximum bending moment and flexural displacement occur at the geometrical center of the plate, where flexural damage would most likely occur. In the cantilever plate, the maximum bending moment and shear force occur at the clamped edge where the flexural displacement is a minimum, so that the damage is usually in the form of a crack along the fixed edge.

The configuration of the cantilever plate is shown in Fig. 2. The dimensions of the plate are 600 mm × 480 mm with 20 mm plate thickness. The finite element model of the plate consists of $15 \times 12 = 180$ equal size square Reissner–Mindlin plate elements. Three d.o.f., which are

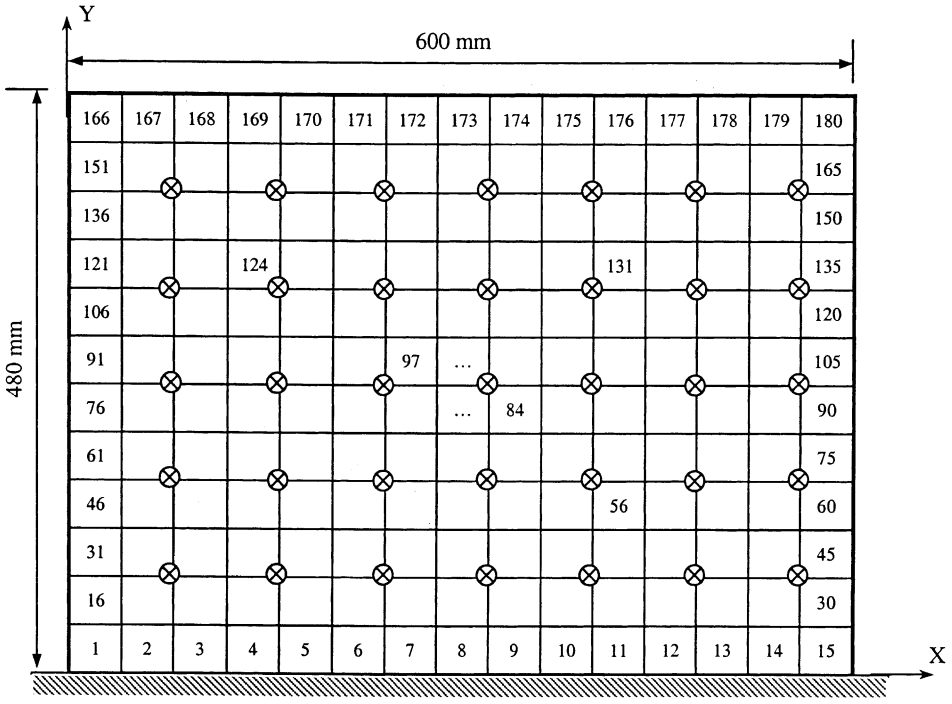

Fig. 2. Finite element model of the cantilever plate; ⊗—gapped grid of measuring points.

translational along the Z-axis and rotational along the X- and Y-axis, are used at each node. The simply supported plate has the same dimensions and finite element mesh as the cantilever plate, except with different boundary conditions.

It is assumed that damage will affect only the stiffness matrix of a structure. The change in the stiffness matrix due to damage is modelled by a reduction in Young's modulus of the corresponding element. The extent of damage is then linearly related to the degree of reduction in the Young's modulus E.

For each damage case, the natural frequencies and corresponding mode shapes are obtained from finite element analysis. The ULS curvatures are calculated separately using Eqs. (6) and (16). Since the three d.o.f.s at each node in the Reissner–Mindlin plate elements are uncoupled, one is offered choices to calculate the translational d.o.f.-based ULS curvature or rotational d.o.f.-based curvatures. The authors' simulation study shows that the latter is more sensitive to local damage and less sensitive to random noise than the former. However, since there is difficulty to measure the rotational d.o.f.s with current dynamic testing technique, only the translational d.o.f. along the Z-axis are used in the paper. Eqs. (7), (17) and (19) are then separately used in the calculation, of damage index based on changes in the ULS curvature and the gapped-smoothing technique. The weights α_{xx}, α_{yy} and α_{xy} are all taken equal to unity. The effectiveness of the methods from central difference, and from the Chebyshev polynomial are compared. The effects of measurement noise, mode truncation, and sensor sparsity on the ULS curvature changes are also studied with particular damage cases.

Table 1
Natural frequencies of the simply supported plate

Mode	Natural frequency (rad/s)			Percentage reduction (%)	
	Intact	Case 1	Case 2	Case 1	Case 2
1	21.324	21.165	21.121	0.751	0.961
2	31.631	31.307	31.572	1.035	0.187
3	36.298	35.858	36.266	1.227	0.088
4	43.094	42.499	42.936	1.400	0.368
5	44.011	43.875	43.670	0.310	0.781

3.1. Simply supported plate

For the four-side simply supported plate, two different damage patterns are simulated to study the capability of the proposed methods for sparsely distributed and closely distributed damage, respectively. Case 1 has 75% damage in element 56, 50% damage in element 131 and 25% damage in element 124. Case 2 has 50% damage in both elements 84 and 97. A comparison of the first five natural frequencies for the intact case and the two damaged cases are shown in Table 1.

3.1.1. Study on truncation effect

As mentioned in Section 2.1, the ULS, as well as the modal flexibility, can be approximately obtained from the few lower modes. However, if too few modes are identified experimentally, the flexibility or ULS from modal parameters will generally appear stiffer than it really is, and consequently affects the results of damage detection. The study on how many modes or what frequency band is sufficient for the modal-based ULS from Eq. (4) leading to reliable damage detection is called truncation effect analysis. Fig. 3 compares the changes in the exact modal flexibility and the changes in the exact ULS due to damage Case 1 with the modal parameters from the first three modes. The exact ULS is calculated using all the modes available in the finite element model. The percentage truncation errors were evaluated as

$$\{e_{ij}\}_{\mathrm{d}u} = \frac{\{\mathrm{d}u_{ij}\}_R - \{\mathrm{d}u_{ij}\}_T}{\max\{\mathrm{d}u_{ij}\}_R} \times 100\%, \tag{20}$$

where $\{\mathrm{d}u_{ij}\}_R$, $\{\mathrm{d}u_{ij}\}_T$ are the changes of the exact ULS and the changes of modal truncated ULS, respectively. Truncation error on the modal flexibility was computed similarly. It can be seen that the ULS converges more rapidly than modal flexibility with the first three lower modes. The truncation errors in ULS are less than 6%, whereas the maximum truncation error in modal flexibility approaches 25%. In the following studies, all the ULS curvatures for the intact and damaged plates are estimated from the first three modes.

3.1.2. Comparison of curvature methods

The changes in the curvature of the uniform load surface for the plate with damage Case 1 are plotted in Fig. 4. Figs. 4(a)–(c), respectively, show the results computed from Eqs. (7) and (17), and from Eq. (19) when there is no information of the intact state. It can be clearly seen that there is a peak located at each damage element. The more severely the element is damaged, the more

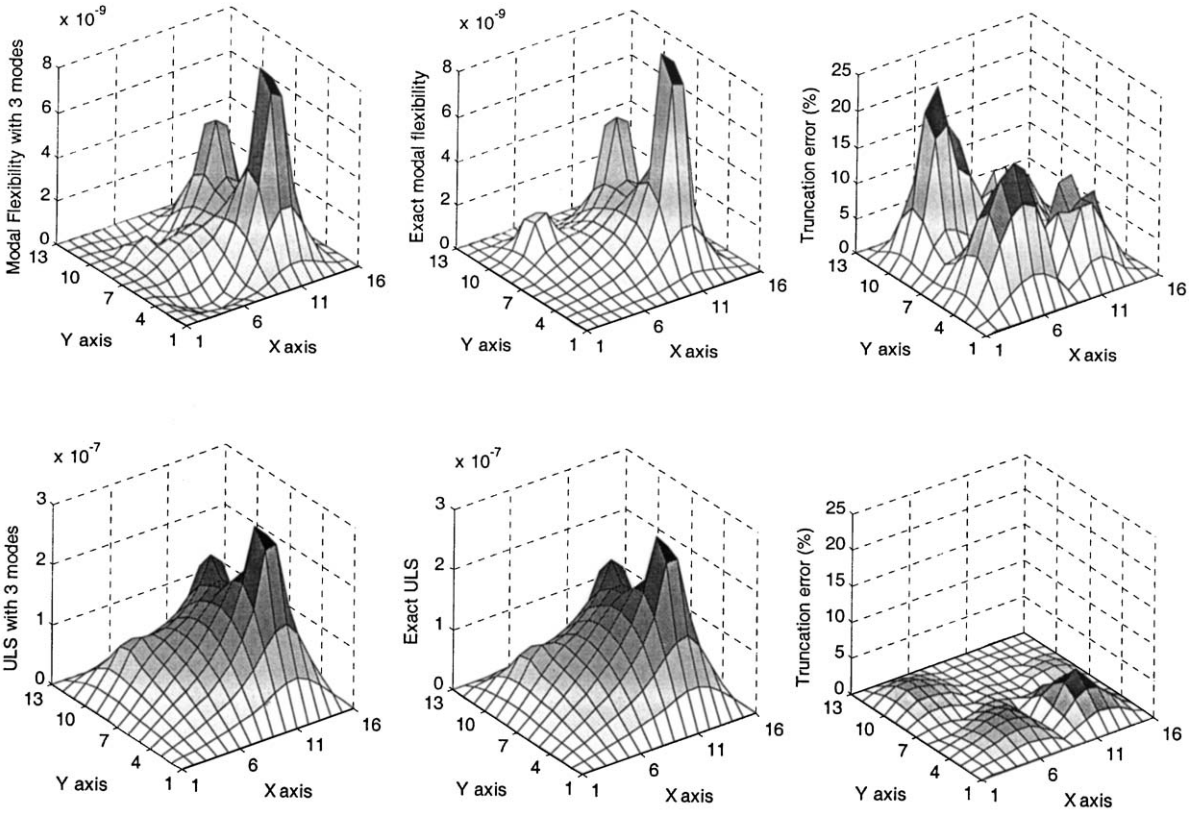

Fig. 3. Comparison of truncation effect on ULS with modal flexibility.

sharp and tall the peak looks. According to Eqs. (7), (17) and (19), the absolute value of the damage indices, or visually the height of the peak, increases exponentially with the change in ULS curvature, and the 25% damage in element 124 shows only a very tiny peak compared with the 75% damage in element 56. Nevertheless, it does not mean the damage with 25% stiffness reduction is the limit the methods can detect. For this case, both the central difference method (Fig. 4(a)) and the Chebyshev polynomial method (Fig. 4(b)) can successfully locate all the three damaged elements, whereas, when prior knowledge on the intact structure is not available, the Chebyshev polynomial method with gapped-smoothing technique failed to locate the damage in element 124.

3.1.3. Resolution of damage localization

It is well known that most damage index methods can localize quite accurately the spatially distributed damage, but suffer from detecting the contiguous multiple damages. Damage Case 2 is specially simulated to study the effectiveness of the proposed methods for closely distributed damages. Fig. 5 shows the results of damage detection for this case. It can be seen that the two damaged elements 84 and 97 are located closely at the center of the plate, and they can be separately detected by inspecting the change in ULS curvature, computed either from central

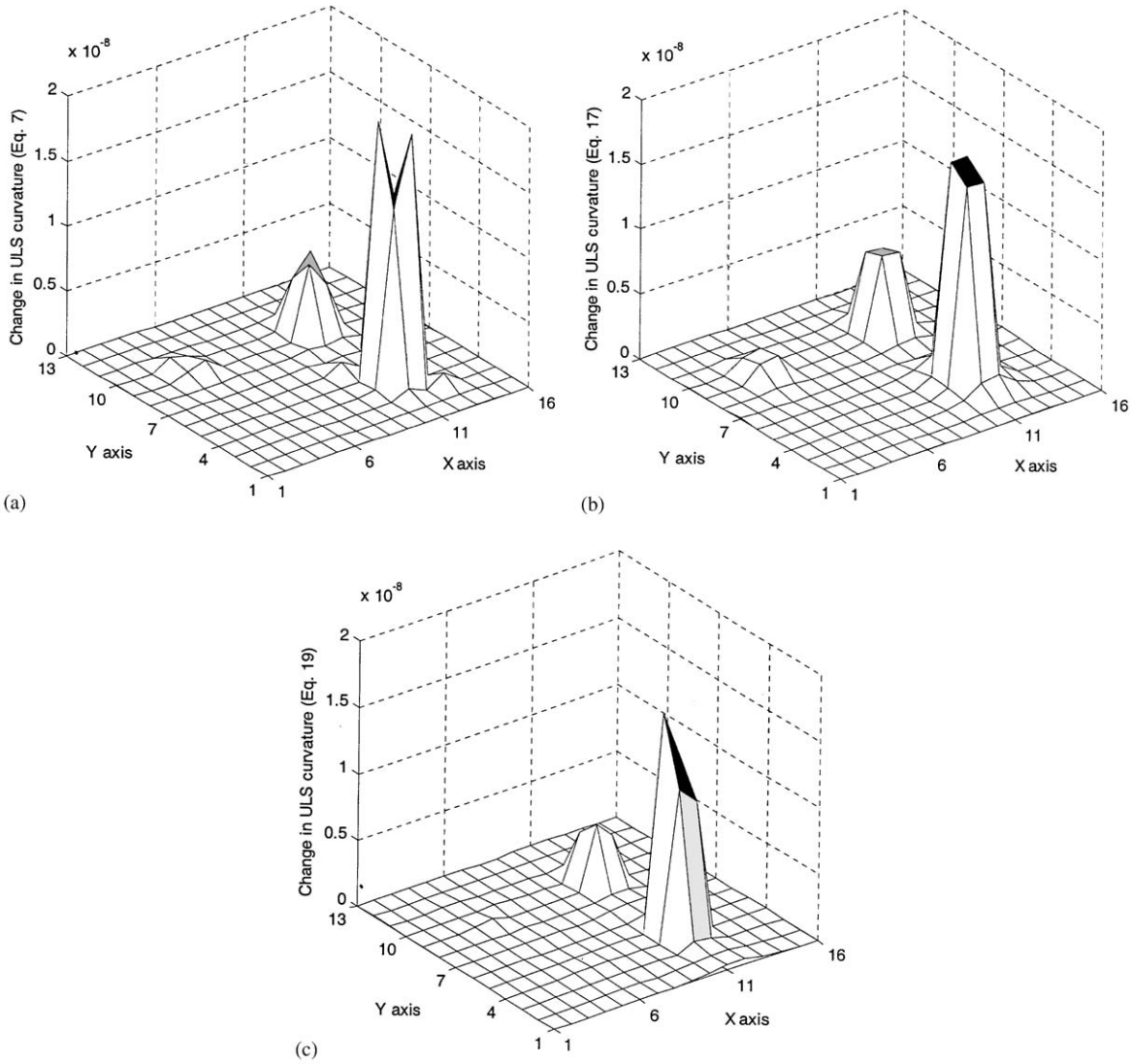

Fig. 4. Damage index map due to damage Case 1: (a) curvature from central difference; (b) curvature from Chebyshev polynomial; (c) curvature from Chebyshev polynomial with gapped-smoothing technique.

difference or by the Chebyshev polynomial. However, when given the modal data for the damaged state only, although the damaged region can be localized from Fig. 5(c), it is hard to tell exactly which element is damaged.

3.2. Cantilever plate

It is always a difficult problem to the damage index methods that a damage near the supported boundary is hard to be identified reliably. For an one-side clamped slab, it is intuitive that the

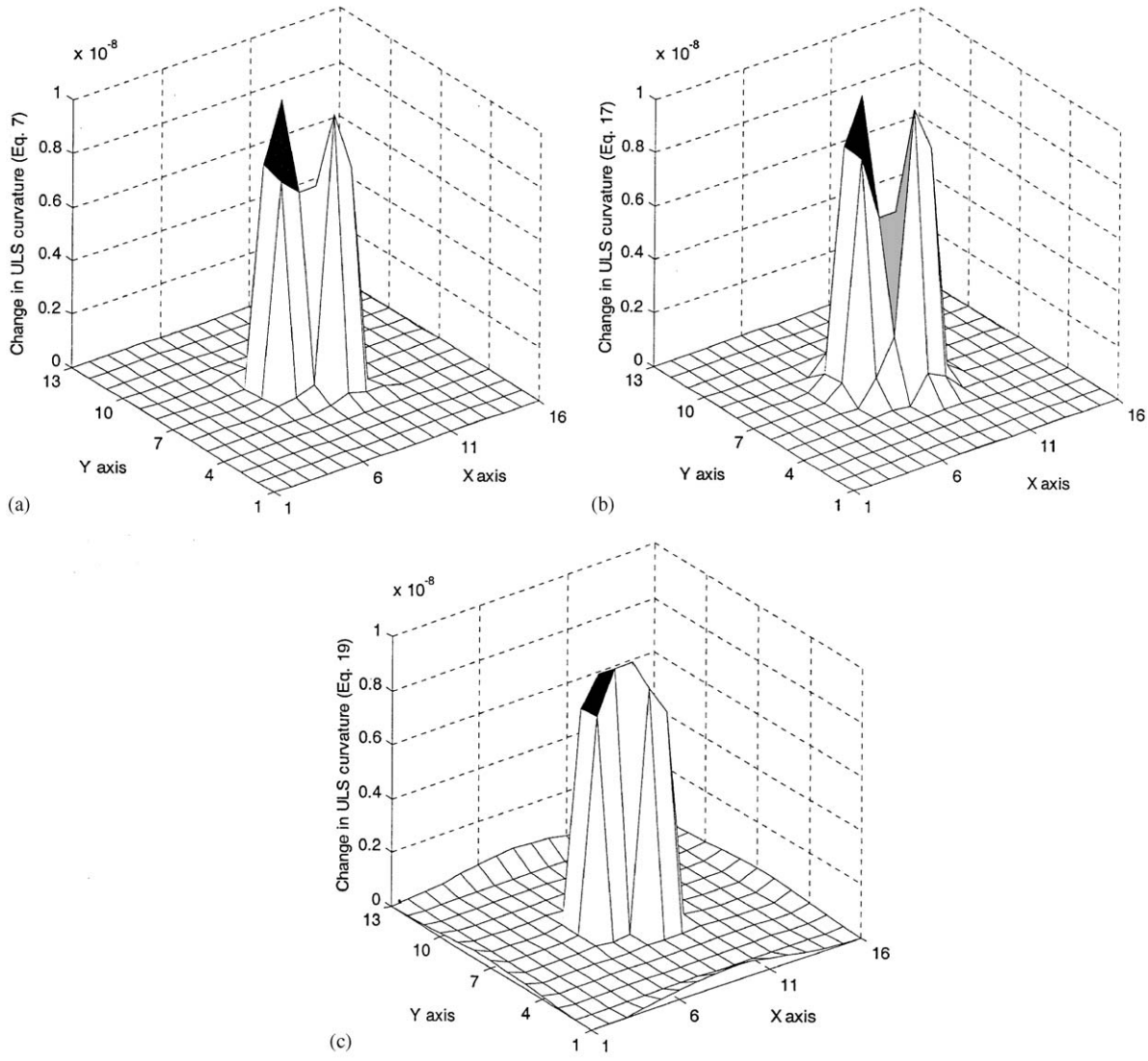

Fig. 5. Damage index map due to damage Case 2—legends similar as Fig. 4.

damage is more likely to develop near and along the fixed edge where the maximum bending moment occurs. Two typical damage cases for the cantilevered slab are simulated. Case 3 has 75% damage in element 15, 50% damage in elements 13 and 14 and 25% damage in element 12. Case 4 has 75% damage in element 8, 50% damage in elements 7 and 9 and 25% damage in elements 6 and 10. The damage in Case 3 starts from one end of the fixed edge and continues along the edge across 4 elements. The damage in Case 4 models a band of damage symmetrically located in the middle and along the fixed edge across 5 elements. The natural frequencies for the intact and damaged structures are listed in Table 2.

Table 2
Natural frequencies of the cantilever plate

Mode	Natural frequency (rad/s)			Percentage reduction (%)	
	Intact	Case 3	Case 4	Case 3	Case 4
1	8.051	7.932	7.879	1.478	2.183
2	11.305	10.987	11.296	2.813	0.080
3	16.561	16.32	16.541	1.455	0.121
4	22.109	21.667	22.105	1.999	0.018
5	24.765	24.442	24.310	1.304	1.872

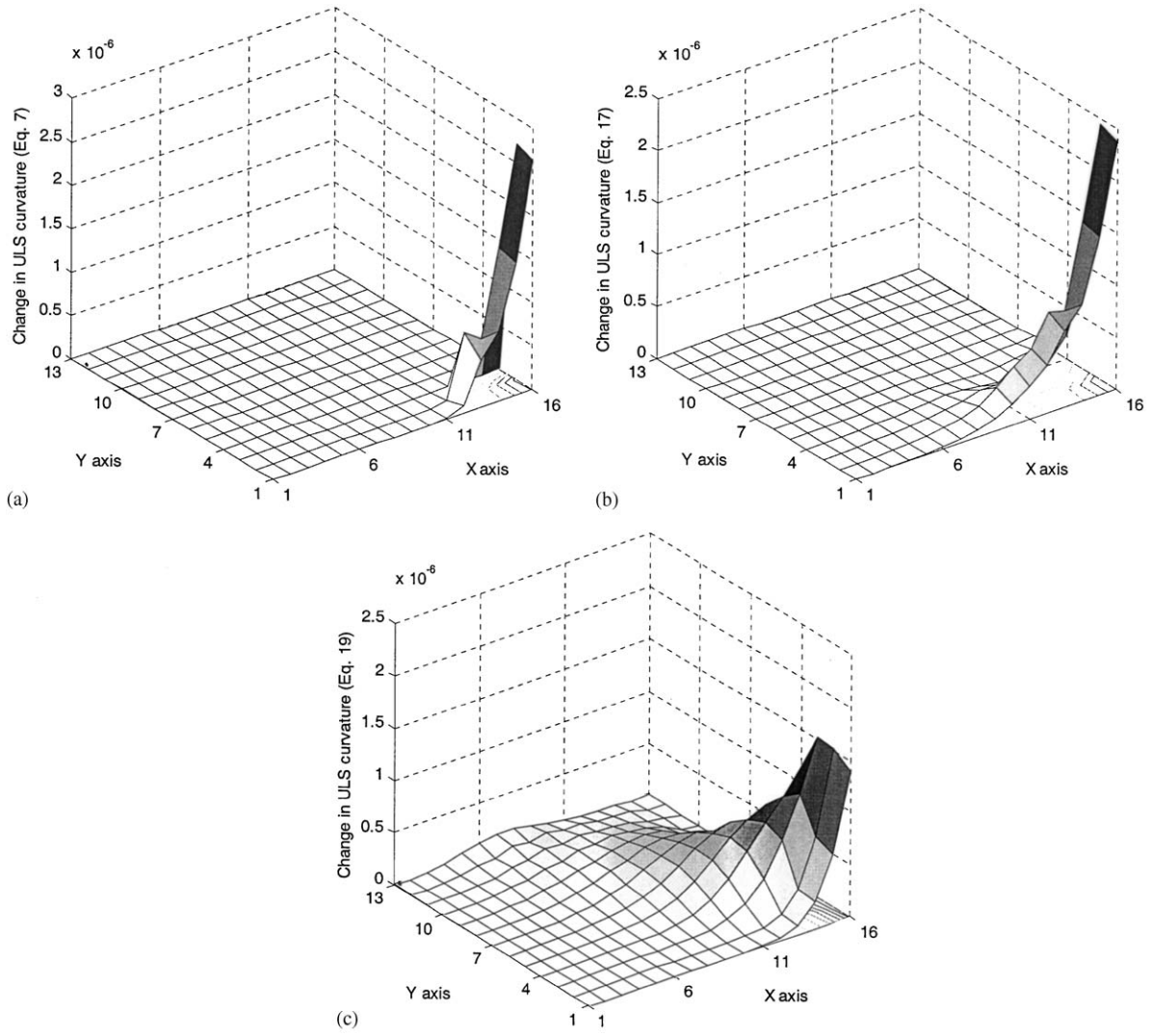

Fig. 6. Damage index map due to damage Case 3—legends similar as Fig. 4.

The results of damage detection for damage Cases 3 and 4 are shown in Figs. 6 and 7, respectively. It can be seen from Fig. 6 that the damage band near the boundary can be detected by inspecting the ULS change calculated by both methods, even without the initial curvature of intact structure. The ULS curvature by Chebyshev polynomial method gives relatively better localization of the damage than those from central difference with a parabolic curve surface compared with a sharp change from central difference method with more than one peak, while the damage location cannot be exactly validated when intact structure curvature is absent. Similar observation can be obtained in Fig. 7.

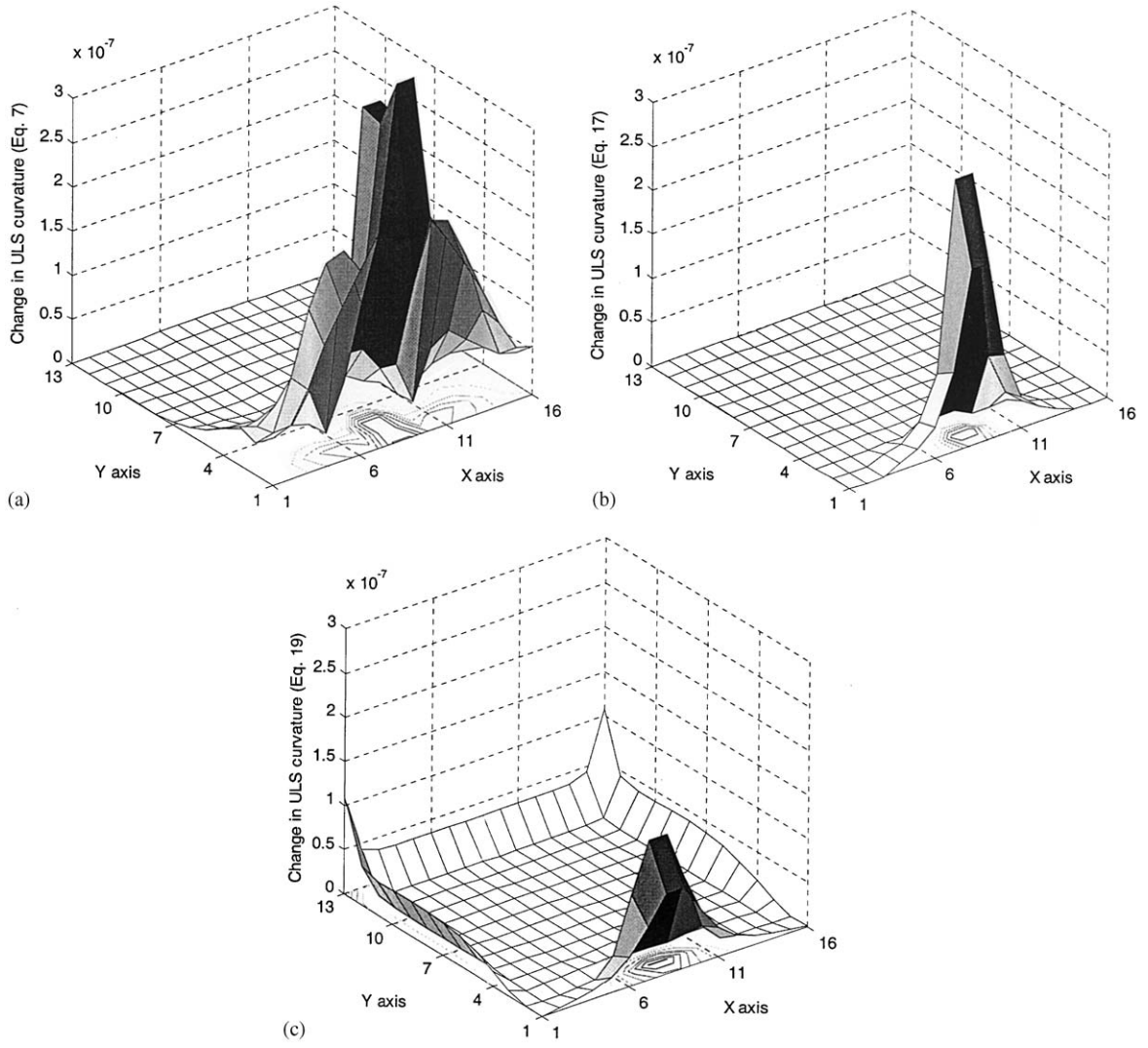

Fig. 7. Damage index map due to damage Case 4—legends similar as Fig. 4.

3.3. Effect of sensor sparsity

In a real experiment it is not practical to have a very fine sensor mesh to measure the dynamic response of all the nodes in the finite element model. To study the effect of sensor sparsity on the proposed methods, the sensor mesh is reduced to 7×5 and the locations are shown in Fig. 2, while the nodes grid of the finite element model is 16×13. The damage Case 1 is studied again with this new sensor grid on the four-side plate. First of all, the sensors are placed at an equal spatial grid as shown in Fig. 2, and the central difference method is applied to estimate the ULS curvature changes due to damage. Then the same number of sensors is placed on the grid points

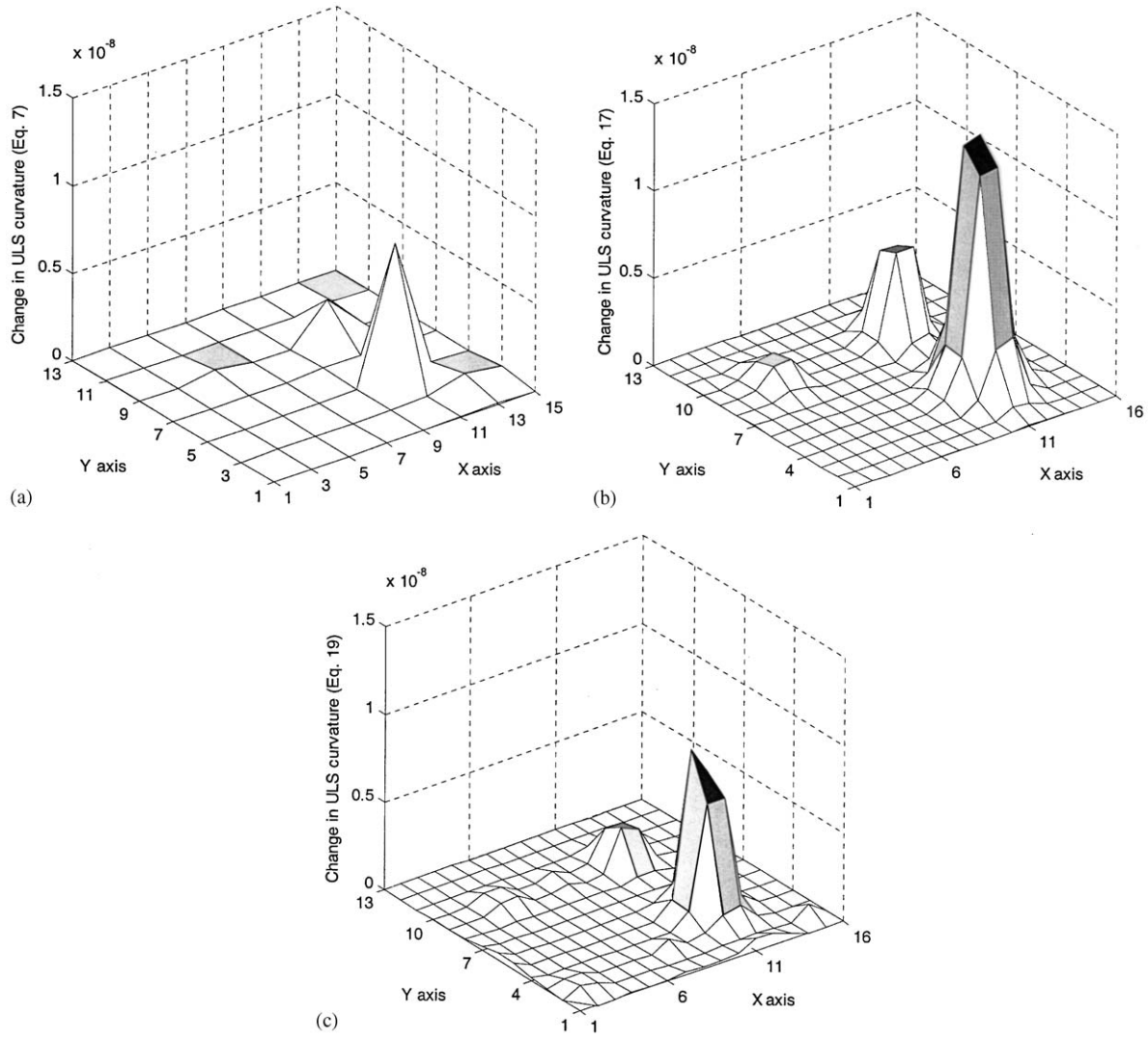

Fig. 8. Damage index map due to damage Case 1 with less dense sensor mesh—legends similar as Fig. 4.

corresponding to the Chebyshev zeros, and the Chebyshev polynomial approximation method is used to calculate the ULS curvature changes in the finite element grid with $M = 7$ and $N = 5$. Chebyshev polynomial method is applied again when the modal data of intact structure is absent, and the ULS curvature for the intact structure is approximated by a cubic smooth polynomial function with the gapped-smoothing technique. Corresponding results of damage detection are plotted in Fig. 8.

It can be seen from Fig. 8(b) that the Chebyshev polynomial method can still localize with confidence all the three damaged element with different extent of stiffness reduction from 25 to 75%. The central difference method fails to detect the damage with 25% stiffness reduction. The absolute values of curvature change at the damaged region degrade dramatically when compared with Fig. 4(b), and the detected area of suspected damaged region is much larger than before. When information on the intact structure is not available, it is fortuitous to find in Fig. 8(c) that the damaged element 124, which is missing in Fig. 4(c), can just be detected even with the polynomial interpolation from the coarse sensor mesh. However, the reason on this observation is unknown.

3.4. Effect of measurement noise

According to Eq. (4), the ULS is estimated from experimentally measured natural frequencies and mode shapes, which are liable to be contaminated by the measurement noise in practice. Thus, in order to take into account the noise in experimentally measured modal parameters, 1% random noise is added into the natural frequencies, and 5% noise is added into the mode shapes. It is assumed that the random noise is uniformly distributed with zero mean and unit variance.

Damage Case 3 in the cantilever plate is studied. Firstly, the ULS curvature change was estimated by central difference method and plotted in Fig. 9(a). It can be seen that the damage index is highly influenced by the measurement noise, and the damaged elements cannot be located from this noisy map of curvature change. To remove the noise effect on the ULS curvature, especially the high peaks near the free edge of the plate, a low order ($M = 6, N = 6$) Chebyshev polynomial function of two variables is used to smooth the oscillatory ULS. The coefficients of this approximation are obtained from Eq. (13). Figs. 9(b) and (c) show the estimated ULS curvature changes as the damage index map, with and without the prior knowledge of intact structure, respectively. It is clear that a low order Chebyshev polynomial approximation on the noisy ULS could dramatically suppress the random noise effect in comparison with Fig. 9(a).

3.5. When the damage changes the boundary condition of the structure

An alternative approach to model damages similar to Cases 3 and 4 is adopted by freeing all the boundary connections within the damage region of the plate. The resulting damage index map looks similar to what we have in the last study. This indicates that the proposed method is applicable even though the damage changes the boundary condition of the structure.

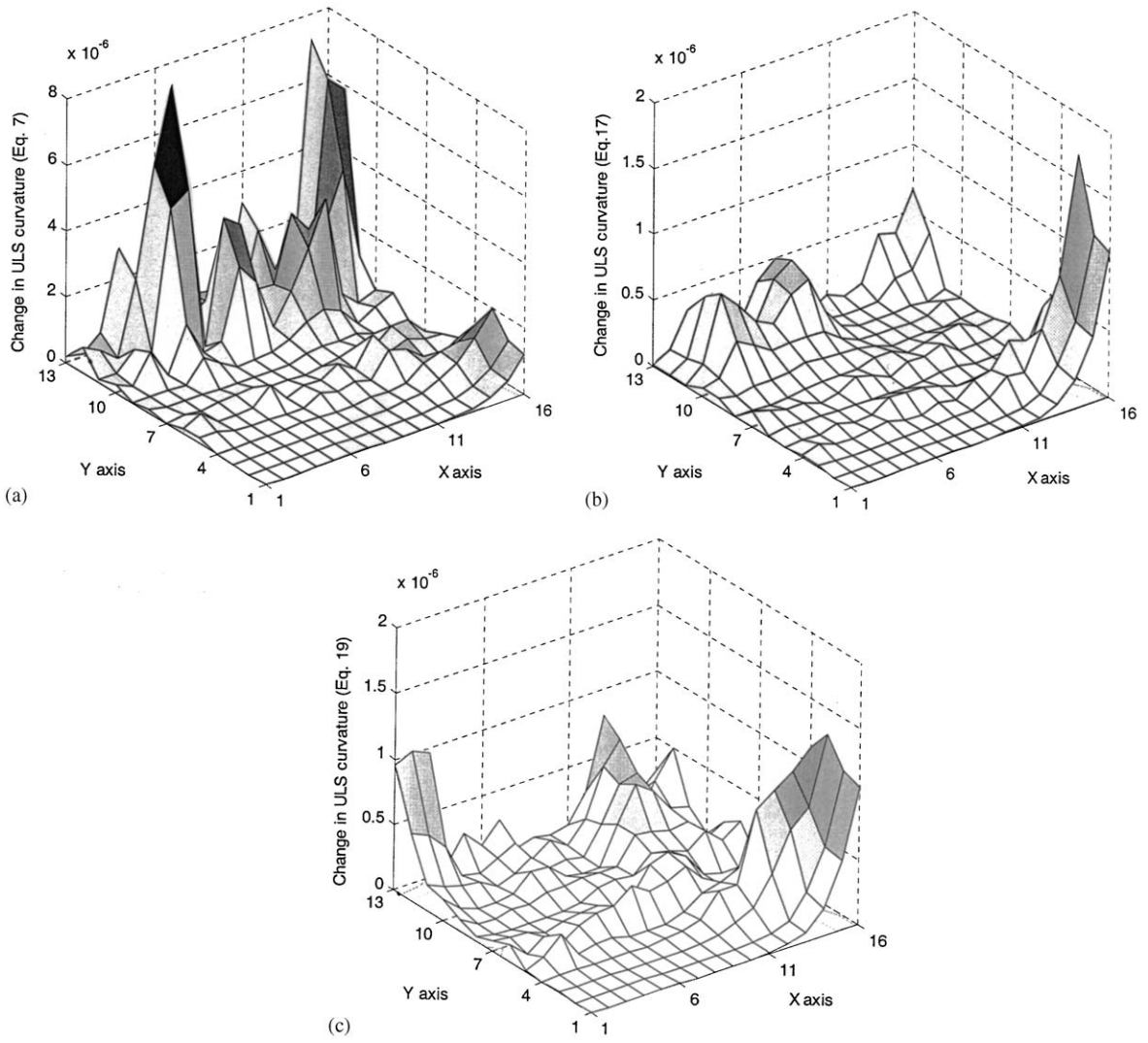

Fig. 9. Damage index map due to damage Case 3 with random noise—legends similar as Fig. 4.

4. Conclusion

In the numerical examples studied, the change in the ULS curvature is found very sensitive to local damages and robust to mode truncation effect. With only the modal data from the first few modes, the ULS curvature can be used to indicate multiple damages quite accurately. It has been checked that when no random noise is present, a damaged element with only 5% reduction in stiffness can be clearly indicated. The effectiveness of this damage index is also demonstrated with different stringent conditions: a simply supported plate with closely distributed damages, and a cantilever plate with near boundary damages.

In comparison to the finite central difference method, a new approach to calculate the ULS curvature is proposed based on Chebyshev polynomial approximation. This method could not only improve the accuracy of the calculated curvature, but also provides more operational flexibility in damage detection process, especially for dealing with the situation of sensor sparsity and the presence of measurement noise. When integrated with the gapped-smoothing technique, the proposed method does not require any prior information of the intact structure.

Acknowledgements

The work described in this paper was supported by a grant from the Hong Kong Polytechnic University Research Funding Project No. G-W092.

References

[1] S.W. Doebling, C.R. Farrar, M.B. Prime, A summary review of vibration-based damage identification methods, *The Shock and Vibration Digest* 30 (2) (1998) 91–105.
[2] F.M. Hemez, C. Farhat, Structural damage detection via a finite element model updating methodology, *Modal Analysis: The International Journal of Analytical and Experimental Modal Analysis* 10 (3) (1995) 152–166.
[3] D.C. Zimmerman, M. Kaouk, Structural damage detection using a minimum rank update theory, *Journal of Vibration and Acoustics* 116 (1994) 222–230.
[4] S.W. Doebling, Minimum-rank optimal update of elemental stiffness parameters for structural damage identification, *American Institute of Aeronautics and Astronautics Journal* 34 (12) (1996) 2615–2621.
[5] P. Cawley, R.D. Adams, The location of defects in structures from measurements of natural frequencies, *Journal of Strain Analysis* 14 (2) (1979) 49–57.
[6] W.M. West, Illustration of the use of modal assurance criterion to detect structural changes in an orbiter test specimen, *Proceedings of the Air Force Conference on Aircraft Structural Integrity*, 1984, pp. 1–6.
[7] N.A.J. Leiven, D.J. Ewins, Spatial correlation of mode shapes, the Coordinate Modal Assurance Criterion (COMAC), *Proceedings of the Sixth International Modal Analysis Conference*, Vol. 1, 1988, pp. 690–695.
[8] Z.Y. Shi, S.S. Law, L.M. Zhang, Damage localization by directly using incomplete mode shapes, *Journal of Engineering Mechanics, American Society of Civil Engineering* 126 (6) (2000) 656–660.
[9] A.K. Pandy, M. Biswas, M.M. Samman, Damage detection from changes in curvature mode shapes, *Journal of Sound and Vibration* 145 (2) (1991) 321–332.
[10] M. Raghavendrachar, A.E. Aktan, Flexibility of multi-reference impact testing for bridge diagnostics, *Journal of Structural Engineering, American Society of Civil Engineering* 118 (1992) 2186–2203.
[11] J. Zhao, J.T. Dewolf, Sensitivity study for vibrational parameters used in damage detection, *Journal of Structural Engineering, American Society of Civil Engineering* 125 (4) (1999) 410–416.
[12] A.K. Pandy, M. Biswas, Damage detection in structures using changes in flexibility, *Journal of Sound and Vibration* 169 (1) (1994) 3–17.
[13] Q. Lu, G. Ren, Y. Zhao, Multiple damage location with flexibility curvature and relative frequency change for beam structures, *Journal of Sound and Vibration* 253 (5) (2002) 1101–1114.
[14] Z. Zhang, A.E. Aktan, Application of modal flexibility and its derivatives in structural identification, *Research in Nondestructive Evaluation* 10 (1) (1998) 43–61.
[15] A. Berman, W.G. Flannely, Theory of incomplete models of dynamic structures, *American Institute of Aeronautics and Astronautics Journal* 9 (1971) 1481–1487.
[16] J.C. Mason, D.C. Handscomb, *Chebyshev Polynomials*, Chapman & Hall/CRC, Boca Raton, FL, 2003, pp. 145–163.
[17] C.P. Ratcliffe, W.J. Bagaria, A vibration technique for locating delamination in a composite beam, *American Institute of Aeronautics and Astronautics Journal* 36 (6) (1998) 1074–1077.